Structural performance of concrete columns confined with circular imbedded GFRP tubes or rings

S. M. Elzeiny and M. S. Issa
Associate Professor, Reinforced Concrete Institute, Housing and Building National Research Center, Giza, Egypt

Abstract

This research work describes the behavior of axially loaded concrete-filled circular imbedded glass fiber-reinforced polymer tubes (GFRP). Ten columns were tested. Five of them had the dimensions of 200*200 mm, and five had the dimensions of 200*250mm. Two samples had tubes of 1300 mm length, two had rings of 250 mm length, two had rings of 20 mm length at every 200 mm, and two had rings of 20 mm length at every 100 mm. Also, two control columns of no GFRP tubes or rings were tested. For all other specimens, the GFRP tubes or rings were imbedded inside the columns. For the case of columns with GFRP tubes, only the concrete section was axially loaded, as the tubes were shorter than the columns. The study revealed that the strength and ductility of concrete columns were generally improved due to confinement using GFRP tubes or rings. The columns with 1300 mm tubes recorded the highest confinement level. Analytical model to predict the entire stress-strain curve of concrete-filled FRP tubes was slightly modified and then verified using the experimental results. The model showed close correlation to the experimental results in the ascending part of the curve. The comparison between the experimental results and those of the analytical models indicated that the model of Fardis and Khalili [Saafi et al., 1999] yields the best prediction of the ultimate compressive confined strength while the model of Karbhari et al. [Saafi et al., 1999] yields the best prediction of the strain at peak confined strength.

Key words: *Columns, Confinement, Imbedded Glass Fiber-Reinforced Polymer Tubes, Rectangular Cross Section, Analytical Models*

1. Introduction

There is a great demand for columns to be constructed using more durable materials which can withstand aggressive corrosive environments. Fiber reinforced polymer composites (FRP) can be used to confine concrete columns, which significantly improves the strength, ductility, and durability. The FRP tubes act as formwork, protective jacket, confinement, and shear and flexural reinforcement. The use of fiber composites for confinement of concrete is a relatively new approach. FRP tubes provide more confinement effect compared to steel tubes due to the possibility of controlling its Poisson's ratio to be smaller than that of steel [Fam and Rizkalla, 2001]. Also, the confining pressure provided by steel tubes has an upper constant value associated with tube yielding, while FRP tubes provide a continuously increasing confining pressure and consequently more ultimate confining strength and ductility [Fam and Rizkalla, 2001]. Generally, concrete filled FRP tubes are used to carry axial compression loads and may be bending moments. Axial loads are either applied to both the concrete core and FRP tube or to the concrete core only for an optimum use of the FRP tube in the

hoop direction for confinement. Comments about the experimental and analytical research related to fiber confined concrete are available in references [Fam and Rizkalla, 2001; Fam and Rizkalla, 2001; and Saafi et al., 1999]. The models originally developed for columns confined with steel tubes are not necessarily valid for columns confined with FRP tubes as the behavior of FRP-confined concrete is different than that of steel-confined concrete. Saafi et al. [Saafi et al., 1999] reported that applying some of the models developed originally for steel-confined concrete to concrete confined with FRP tubes may result in over-estimating the strength, thus leading to unsafe design [Fam and Rizkalla, 2001a; Fam and Rizkalla, 2001b; Saafi et al., 1999; Mander et al., 1988; Karabinis and Kiousis, 1996; Fafitis and Shah, 1985; Priestly and Park, 1987; Sheikh and Yeh, 1986; Abdel-Halim and Abu-Lebdeh, 1989; Sayed, 2005a; and Sayed, 2005b].

2. Research significance

Environmental factors such as temperature, fire, radiation, and humidity can affect structural integrity and long-term performance of concrete columns. The encased concrete by FRP shows an increase in the strength and ductility of columns due to confinement. Cost savings are realized by reducing the cross-sectional area required for the same design load. The performance of concrete columns confined with circular imbedded glass fiber-reinforced polymer tubes, including experimental and analytical work, is presented in this paper. The applicability of some design models for FRP tube-confined concrete is discussed. The FRP tube is placed inside the column to be protected from possible fire by the concrete cover.

3. Experimental program

Ten reinforced concrete columns were casted. The length of each column is 1500 mm. Five columns had a cross-section of 200*200 mm, and five had a cross-section of 200*250 mm. Each column was reinforced with four deformed bars of 10 mm diameter and of grade 360/520. Plain mild steel stirrups of 8 mm diameter, 240/350, were used with spacing as shown in Figs. (1) and (2). GFRP tubes or rings were placed inside the stirrups for protection of possible fire. Columns C0-20 and C0-25 were control columns without any GFRP. Columns C130-20 and C130-25 had 1300 mm GFRP pipe inside the stirrups. Four GFRP rings of length 250 mm each were installed in columns C25-20 and C25-25 on intervals as shown in Figs. (1) and (2). The rest four columns had GFRP rings of 20 mm length located inside the stirrups on spacing as shown in Fig. (2).

Fig. (1): GFRP Tubes and Rings Placed Inside the Reinforcement Cages. (Four Columns Stacked Horizontally on Top of Each Other Are Shown)

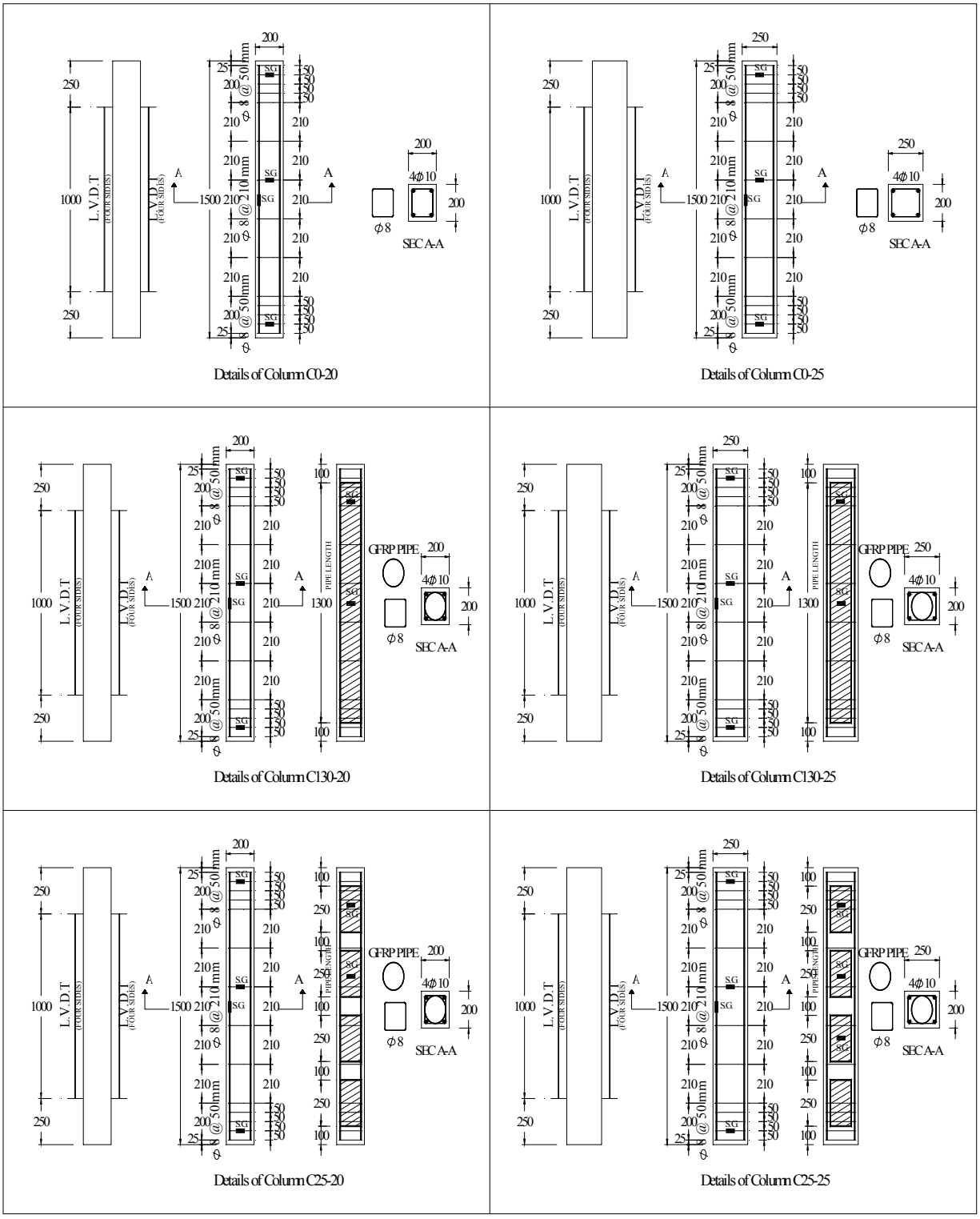

Fig. (2): Details of Tested Columns.

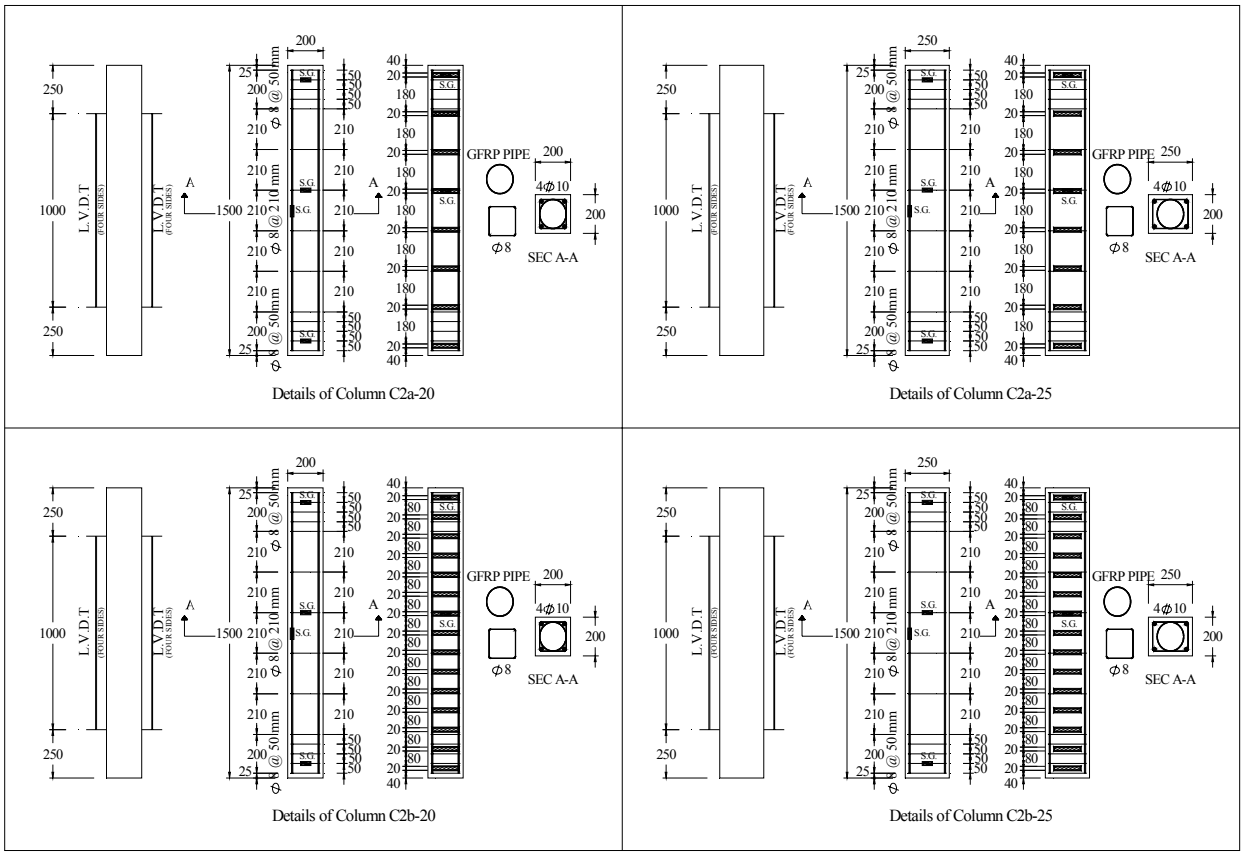

Fig. (2): Details of Tested Columns (Continued).

4. Materials

The mechanical and physical properties of the used GFRP tubes and rings were measured by the authors. Table (1) summarizes their thickness, internal diameter, external diameter, hoop tensile strength and modulus of elasticity. The GFRP properties in the hoop direction were obtained after performing tension test using the split-disk method. In this method, two semicircular steel plates were used to apply the tension force to the GFRP ring. Strain gages were attached in the hoop direction. Thus, the stress-strain curve in the hoop direction was obtained. The average 28-day standard cube (150*150*150 mm) compressive strength (f_{cu}) is 32.23 MPa. The equivalent standard cylinder (150*300 mm) compressive strength (f'_c) is 25.78 MPa. The concrete mix used for casting all the columns was produced from ordinary Portland cement, natural sand and crushed dolomite with a maximum size of 10 mm. The columns were demolded after 24 hrs from casting, covered with wet burlap and stored under the laboratory conditions for 28 days before proceeding to testing stage.

Table (1): Properties of GFRP Tubes and Rings.

Thickness (t) (mm)	Internal Diameter (mm)	External Diameter (mm)	Hoop Tensile Strength (f_{com}), (MPa)	Modulus of Elasticity (E_s), (GPa)
8.75	150.4	167.9	171.4	56.8

5. Instrumentation and testing

Four linear variable displacement transducers (LVDTs) were attached on a length equal to 1000 mm of the four faces of each column. This pattern of gages allows for accurate axial strain measurements and traces any unintended eccentricity during loading. Strain gages (S.G.) of 10 mm length were installed at the stirrups and middle of longitudinal reinforcement. Strain gages of 10 mm length were also installed on the outside surface of the tubes or rings near the end of the tube or at an end ring and at the middle height of the tube or at middle ring to measure the strain in the hoop direction. All the columns were tested using 500-ton testing machine, see Fig. (3). A thin layer of plaster was placed between the end faces of the column and both the loading and supporting steel plates to insure uniform distribution of the applied pressure.

Fig. (3): General View of Test Setup.

6. Test results

6.1. Mode of failure

During testing, the columns surfaces were observed in order to follow the development and the propagation of cracks. The appearance of these cracks was always the sign that column attained the failure state. The failure mechanisms of the columns with and without the impeded GFRP tubes or rings were the same. The typical damage sequence for concrete was as follows: inclined cracks occurred at the beginning of the upper or lower part of the column and with increasing the applied load cracks become wider and cover spalled off. For column C0-20, major inclined cracks formed from the lower part to one of the column sides till complete failure at load equaled to 1034.5 kN. For the column C0-25 the same failure mechanisms as column C0-20 was occurred except that failure occurred at column upper third at load equaled to 1252.9 kN. For the rest of the columns which had an impeded GFRP tubes or rings, similar failure mechanisms to columns C0-20 and C0-25 were occurred at different positions. Fig. (4) shows the crack patterns for all the tested columns.

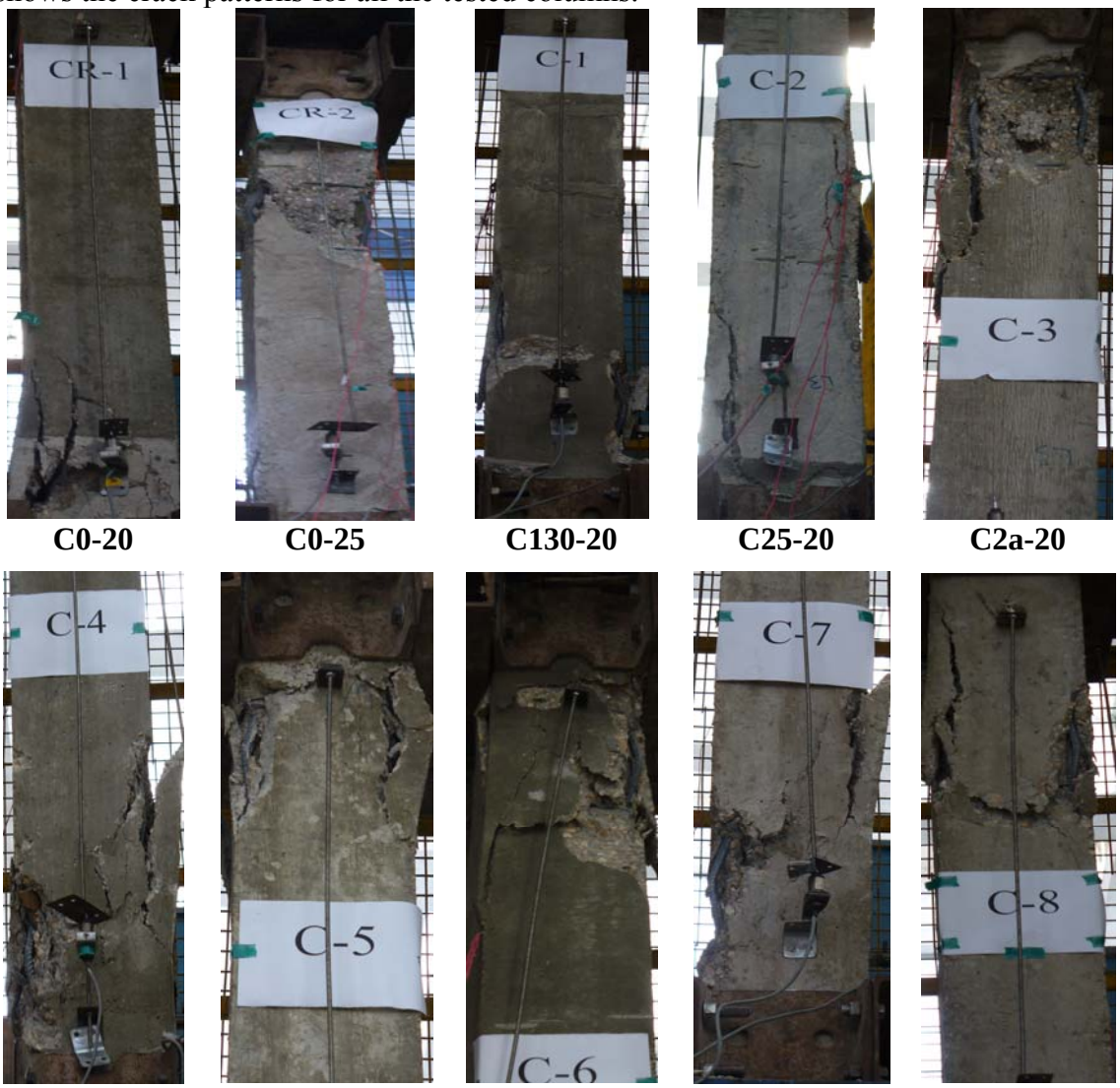

C0-20 **C0-25** **C130-20** **C25-20** **C2a-20**

C2b-20 **C130-25** **C25-25** **C2a-25** **C2b-25**

Fig. (4): Failure Patterns of Tested Columns.

6.2. Axial Stress-Strain Behavior

Figs. (5) and (6) show the axial stress-axial strain curves for the tested columns. All the curves start with linear part where the slope of the confined concrete is close to that of the unconfined concrete. At stress levels near the ultimate stress of unconfined concrete, the curves start to bend indicating that concrete had cracked and consequently the GFRP started its confining effect because the lateral expansion of the concrete core became greater than that of the GFRP tube or rings.

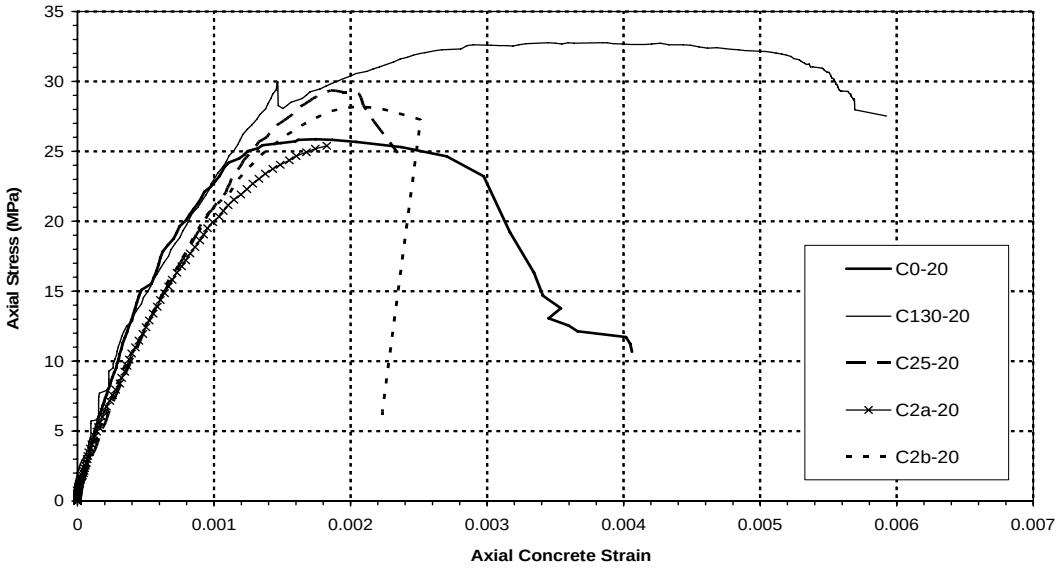

Fig. (5): Axial Stress-Strain Curves for the Columns of 200*200 mm Cross Section.

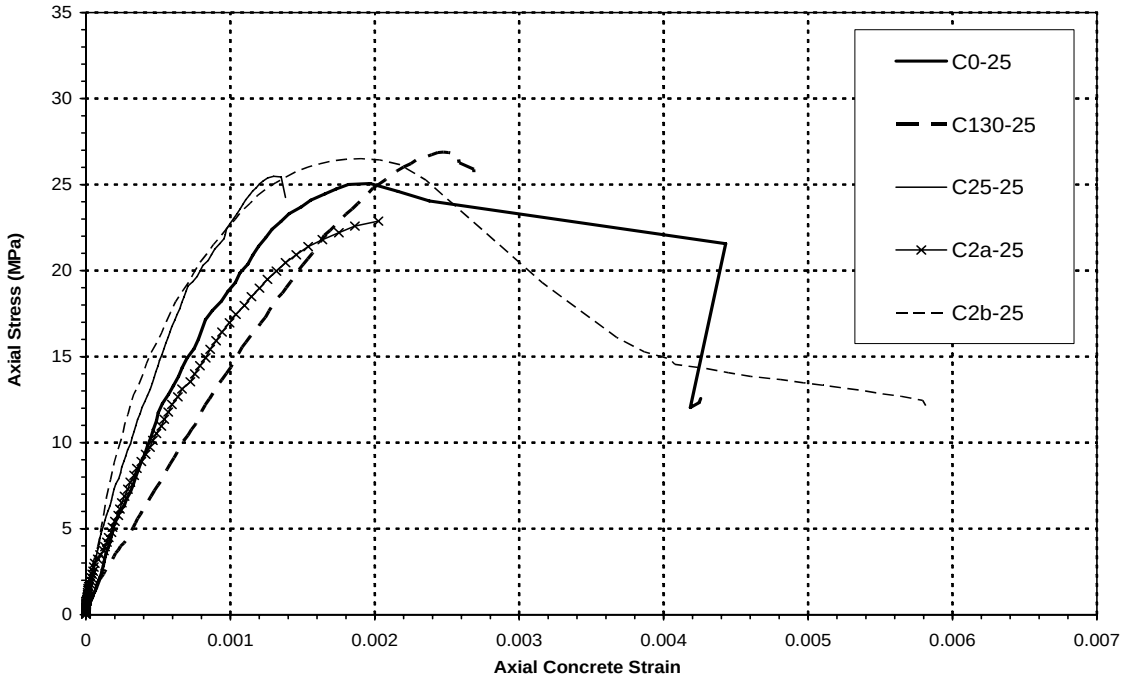

Fig. (6): Axial Stress-Strain Curves for the Columns of 200*250 mm Cross Section.

6.3. GFRP and Reinforcement Strains

Sample of the measured longitudinal steel strain is shown in Fig. (7) for column C130-25. The maximum attained strain is 0.019 which indicates that the longitudinal steel has yielded. Fig. (8) shows sample of the measured strain in the hoop direction for the middle of the GFRP tube used to confine column C130-25. The recorded strain at the maximum attained axial load by the column is 0.001 approximately.

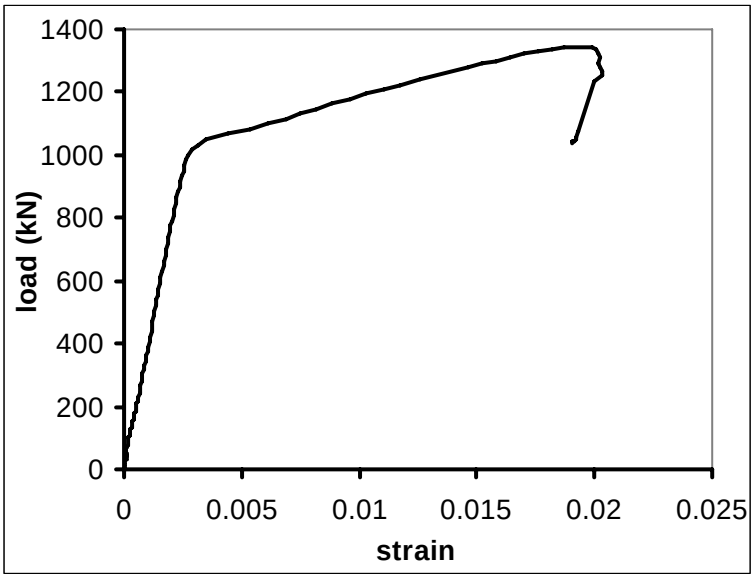

Fig. (7): Axial Load-Longitudinal Steel Strain for Specimen C130-25.

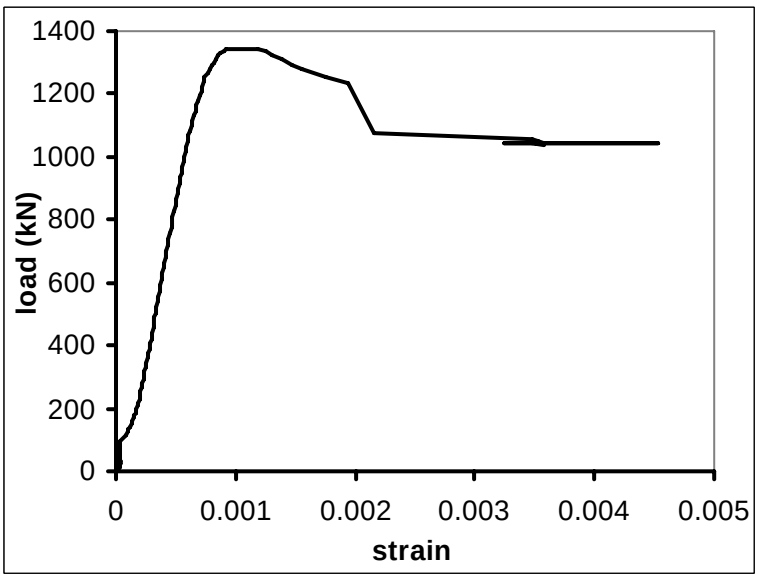

Fig. (8): Axial Load-Hoop Strain of the GFRP Confining Tube of Column C130-25

7. Discussion of test results

7.1. Strength Measures

From Table (2), where the axial stress f'_{cc} was calculated by dividing the ultimate axial load on the actual cross-sectional area of the columns, the maximum increase in

the ultimate compressive strength was attained by column C130-20 which had a continuous FRP pipe of length 1300 mm. The increase in strength was 26.66%. The column C2a-20, which had GFRP rings of length 20 mm on 200 mm intervals, recorded no increase in the strength. This is because the GFRP rings and stirrups had the same spacing. Thus the effect of the GFRP rings was limited. The percentage of the increase in the strength with confinement for the 200*250 mm columns was generally small compared to that of the 200*200 mm columns. This is because the dimensions of the confined core for both the 200*200 mm columns and the 200*250 mm columns was the same and the unconfined core for the 200*250 mm columns are bigger than the unconfined core of the 200*200 mm columns. Also similar dimensions for the GFRP tubes and rings were used for both types of columns.

7.2. Ductility

The value of the measured strain at beak confined strength ε'_{cc} is an indication to ductility. The higher values for ε'_{cc} indicate higher ductility. As shown from Table (2), the maximum percentage for the strain increase was obtained by column C130-20 and is equal to 106.32%. While the percentage for the increase in the strain for column C130-25 was 25.38%. Generally, for the confined 200*250 mm columns, lesser ductility is recorded. This is due to the fact that the dimensions of the unconfined zone for the 200*250 mm columns are bigger than the unconfined zone of the 200*200 mm columns. Thus, large proportion of the 200*250 mm columns lies outside the core confined with GFRP tubes or rings.

Table (2): Experimental Results.

Column	f'_{cc} exp. (MPa)	Strength Change%	ε'_{cc} exp.	Strain Change%
C0-20	25.88	---	0.00174	---
C130-20	32.78	+26.66	0.00359	+106.32
C25-20	29.35	+13.41	0.00185	+6.32
C2a-20	25.55	-1.28	0.00190	+9.20
C2b-20	28.18	+8.89	0.00210	+20.69
C0-25	25.06	---	0.00197	---
C130-25	26.88	+7.26	0.00247	+25.38
C25-25	25.44	+1.52	0.00135	---
C2a-25	22.98	-8.30	0.00220	+11.68
C2b-25	26.50	+5.75	0.00190	---

7.3. Confinement Measures

As explained in references [Karabinis and Kiousis, 1996; Fafitis and Shah, 1985; Priestly and Park, 1987; Sheikh and Yeh, 1986; and Abdel-Halim and Abu-Lebdeh, 1989], the column strength is evaluated using two measures. The first measure is the

effective confinement (K_s) which is defined as the ratio between the confined core, inside the GFRP tube or rings, strength (f_{cc}) to the unconfined concrete compressive strength (f_{co}). The unconfined concrete compressive strength (f_{co}) is taken equal to 0.70 times the standard cube compressive strength (f_{cu}) as suggested in reference [Karabinis and Kiousis, 1996]. The confined core strength (f_{cc}) is equal to the load carried by the concrete core only ($P_{c\ max}$) divided by the area of the confined core (A_{co}). Pc max equals to the total attained experimental load (P_{max}) minus the load which can be resisted by the vertical reinforcement (P_{st}) and minus the load resisted by the concrete cover, which is f_{co} times the area of the cover. The second measure for the column strength is the gain of the confined core strength (Δf_c) which is the difference between the confined core strength (f_{cc}) and the unconfined core strength (f_{co}). As can be seen in Table (3), both the strength measures are increased when confining using GFRP tubes or rings, with the exception of specimens C2a-20 and C2a-25 which had rings of 200 mm spacing. The maximum increase is recorded for specimens C130-20 and C130-25. The percentage of increase for column C130-20 in K_s and Δf_c was 53.5 and 233.5, respectively. Similarly, the percentage of increase for column C130-25 was 17.2 and 82.8, respectively.

Table (3): Effective Confinement Factor and Gain in Strength.

Column	$P_{max,exp}$ (kN)	$P_{c\ max}$ (kN)	f_{cc} (MPa)	K_s	Δf_c (MPa)
C0-20	1034.9	518.6	29.2	1.29	6.65
C130-20	1310.7	794.4	44.7	1.98	22.18
C25-20	1174.1	657.8	37.0	1.64	14.49
C2a-20	1022.1	505.8	28.5	1.26	5.93
C2b-20	1127.4	611.1	34.4	1.53	11.86
C0-25	1252.9	511.0	28.8	1.28	6.22
C130-25	1344.4	602.5	33.9	1.50	11.37
C25-25	1272.1	530.2	29.9	1.32	7.3
C2a-25	1149.4	407.5	23.0	1.01	0.39
C2b-25	1325.3	583.4	32.9	1.46	10.30

8. Analytical analysis

8.1. Confinement models

8.1.1. Model (1): confinement model by Fam & Rizkalla, 2001 with some modifications,

Mander et al., 1988 proposed a stress-strain approach for predicting the behavior of confined concrete subjected to axial compressive stresses. This model is based on a constant confining pressure σ_R .

The axial stress of the confined concrete (f_{cc}) at any given strain (ε_{cc}) is,

$$f_{cc} = \frac{f'_{cc} X r}{r - 1 + X^r} \quad (1)$$

$$X = \frac{\varepsilon_{cc}}{\varepsilon'_{cc}} \quad (2)$$

$$r = \frac{E_{co}}{E_{co} - E_{\sec}} \quad (3)$$

Where f'_{cc} = Peak confined strength.

$\varepsilon_{cc}^{'}$ = Strain at peak confined strength.

E_{co} = Tangent elastic modulus of unconfined concrete.

$= 4400\sqrt{f_{cu}}$ MPa.

$E_{\sec}$ = Secant modulus of confined concrete.

$= \frac{f_{cc}^{'}}{\varepsilon_{cc}^{'}}$

The peak confined strength ($f_{cc}^{'}$) is,

$$f_{cc}^{'} = f_{c}^{'}(2.254\sqrt{1+\frac{7.94\sigma_R}{f_{c}^{'}}} - 2\frac{\sigma_R}{f_{c}^{'}} - 1.254) \quad (4)$$

Where $f_{c}^{'}$ = Peak unconfined strength.

σ_R = Constant lateral confining pressure.

The above equation will be used in the following sections when deriving the axial stress-strain curves for the columns confined with long GFRP tube (columns C130-20 and C130-25). For the rest of the GFRP confined columns (columns C25-20, C25-25, C2a-20, C2a-25, C2b-20 and C2b-25), the following equation is to be used

$$f_{cc}^{'} = f_{c}^{'} + 10 * \sigma_R \quad (5)$$

The peak confined strain ($\varepsilon_{cc}^{'}$) is,

$$\varepsilon_{cc}^{'} = \varepsilon_{c}^{'}[1 + 5(\frac{f_{cc}^{'}}{f_{c}^{'}} - 1)] \quad (6)$$

Where $\varepsilon_{c}^{'}$ = Strain at peak unconfined strength.

= 0.002

In the case of confined columns using FRP tubes, the confining pressure is continuously increasing with loading due to the linear characteristics of the materials of the FRP tube. Fam & Rizkalla, 2001 defined the variable confining pressure as follows:

Consider a concrete cylinder subjected to axial strain ε_{cc}. The radial displacement (U_R) where the lateral expansion is allowed can be evaluated as

$$U_R = \upsilon_c R \varepsilon_{cc} \quad (7)$$

Where υ_c = Poisson's ratio for concrete.

= 0.20

R = The radius of the concrete cylinder or column.

The radial displacement (U_R) where the external radial stress (σ_R) exists can be calculated as:

$$U_R = \frac{1-\upsilon_c}{E_{co}} R\sigma_R \quad (8)$$

Consider a thin FRP tube subjected to lateral confining pressure (σ_R), and not subjected to direct axial strain loading, the radial displacement of the tube (U_R) is:

$$U_R = \frac{\sigma_R R^2}{E_s t} \quad (9)$$

Where E_s = The elastic modulus of the tube in the hoop direction.

R = The average radius of the tube.

t = The wall thickness.

Now, consider the concrete cylinder placed inside the thin FRP tube where only the concrete core is subjected to uniform axial strain loading (ε_{cc}). As the outward radial displacement of the core due to both the axial strain ε_{cc} and the radial pressure σ_R must be equal to the outward radial displacement of the tube due to the same radial pressure σ_R, subtracting equation (8) from equation (7) and equating with equation (9), the radial stress can be calculated at any axial loading from the following equation:

$$\sigma_R = \frac{\upsilon_c}{\frac{R}{E_s t} + \frac{1-\upsilon_c}{E_{co}}} \varepsilon_{cc} \tag{10}$$

8.1.2. Model (2): confinement model by Fardis and Khalili as reported in reference [Saafi et al. 1999],

Fardis and Khalili [Saafi et al., 1999] proposed the following equations for the prediction of strength of concrete-filled glass FRP tubes.

$$f_{cc}^{'} = f_c^{'}[1 + 4.1\frac{f_{com} t}{d f_c^{'}}] \tag{11}$$

$$\varepsilon_{cc}^{'} = 0.002 + 0.001\frac{E_s t}{d f_c^{'}} \tag{12}$$

Where f_{com} = The tensile strength of the composite (hoop stress).

d = The concrete core diameter.

8.1.3. Model (3): confinement model by Karbhari et al. as reported by Saafi et al., 1999,

$$f_{cc}^{'} = f_c^{'}[1 + 2.1\left(\frac{2tf_{com}}{df_c^{'}}\right)^{0.87}] \tag{13}$$

$$\varepsilon_{cc}^{'} = 0.002 + 0.01\frac{2tf_{com}}{df_c^{'}} \tag{14}$$

8.1.4. Model (4): confinement model by Mander et al., 1988 after some modifications which are reported by Safi et al., 1999,

$$f_{cc}^{'} = f_c^{'}[-1.25 + 2.25\sqrt{1 + \frac{7.94}{f_c^{'}}\frac{2tf_{com}}{d-2t}} - \frac{2}{f_c^{'}}\frac{2tf_{com}}{d-2t}] \tag{15}$$

$$\varepsilon_{cc}^{'} = 0.002[1 + 5(\frac{f_{cc}^{'}}{f_c^{'}} - 1)] \tag{16}$$

8.1.5. Model (5): confinement model by Miyauchi et al. as reported by Saafi et al., 1999,

$$f_{cc}^{'} = f_c^{'}[1 + 3.5\frac{2tf_{com}}{df_c^{'}}] \tag{16}$$

$$\varepsilon_{cc}^{'} = 0.002\left[1 + 10.6\left(\frac{2tf_{com}}{df_c^{'}}\right)^{0.373}\right] \tag{17}$$

The equations of model (1) of Fam and Rizkalla as slightly modified above were used to predict the axial stress-strain curve of specimens confined with GFRP, as shown in

Fig.(9). It is clear from the figure that the ascending parts of the predicted curves are close to the experimental result. The peak confined strength ($f_{cc}^{'}$) and the corresponding strain ($\varepsilon_{cc}^{'}$) were calculated for specimen C130-20 using the equations of the different confinement models, which were explained before, and the results are given in Tables (4) and (5), respectively. The $f_{cc}^{'}$ and $\varepsilon_{cc}^{'}$ predictions for specimen C130-25 are identical to those of specimen C130-20 because similar GFRP tube-diameter was used for the confinement of both specimens. When calculating the peak confined strength and the strain at peak confined strength, the value of fcom was substituted for using 0.4*the value in Table (3). This is because the recorded strain for the GFRP tube in the hoop direction for this type of tubes an for this type of tests produces limited hoop stress. As shown in Table (4), model 2 of Fardis and Khalili [Saafi et al., 1999] gave the best prediction for the peak confined strength. However, for the corresponding strain, model 3 of Karbhari et al. [Saafi et al., 1999] yielded the best estimate of the strain at peak confined strength.

Table (4): Comparison for the Predictions of Peak Confined Strength.

Column	$f_{cc}^{'}$ exp (MPa)	$f_{cc}^{'}$, MPa	error, %	$f_{cc}^{'}$, MPa	error, %	$f_{cc}^{'}$, MPa	error, %	$f_{cc}^{'}$, MPa	error, %
		Model 2		Model 3		Model 4		Model 5	
C130-20	32.78	42.1	28.6	45.3	38.2	62.5	90.7	53.7	63.8

Table (5): Comparison for the Predictions of Ultimate Strain.

Column	$\varepsilon_{cc}^{'}$ exp	$\varepsilon_{cc}^{'}$	error, %	$\varepsilon_{cc}^{'}$	error, %	$\varepsilon_{cc}^{'}$	error, %	$\varepsilon_{cc}^{'}$	error, %
		Model 2		Model 3		Model 4		Model 5	
C130-20	0.00359	0.1301	3524	0.0051	42.1	0.0162	351.3	0.0157	337.3

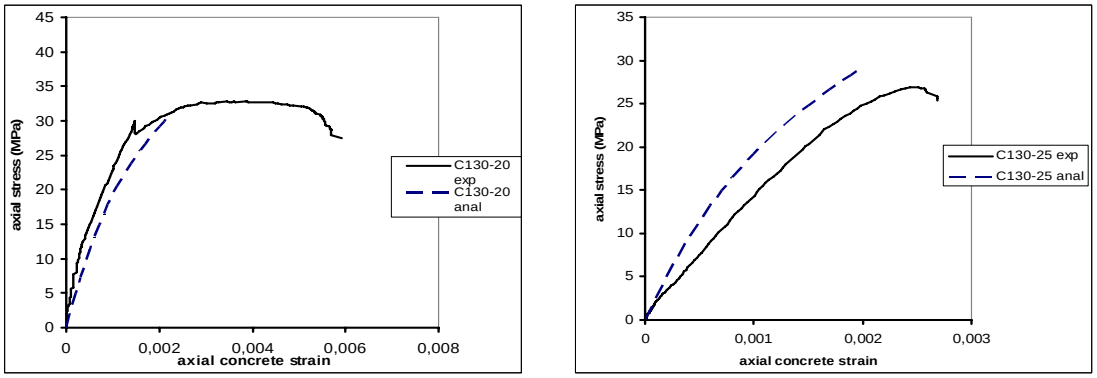

Specimen C130-20 Specimen C130-25

Fig. (9): Analytical Modeling for the Axial Stress-Strain

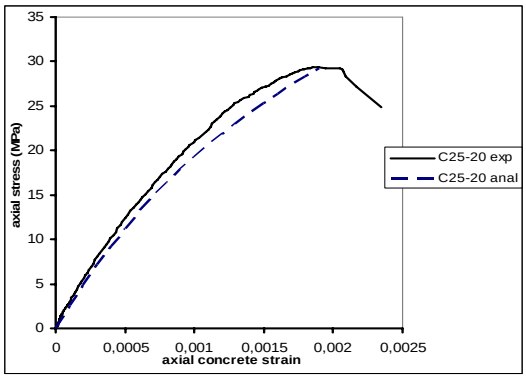

Specimen C25-20

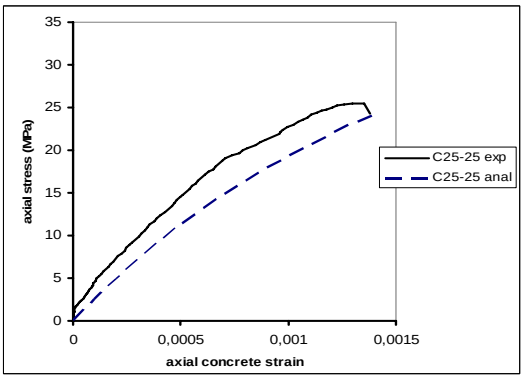

Specimen C25-25

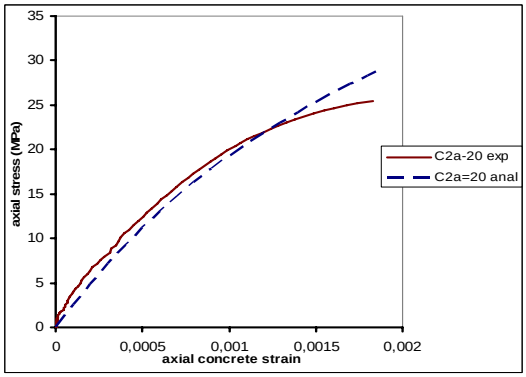

Specimen C2a-20

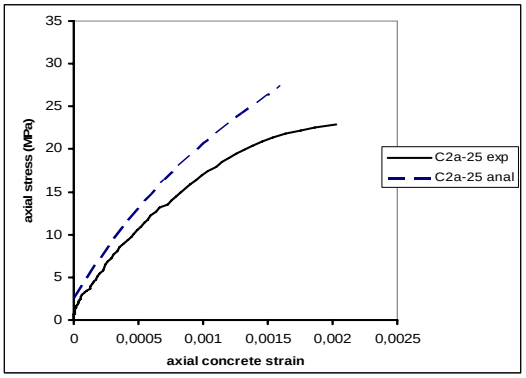

Specimen C2a-25

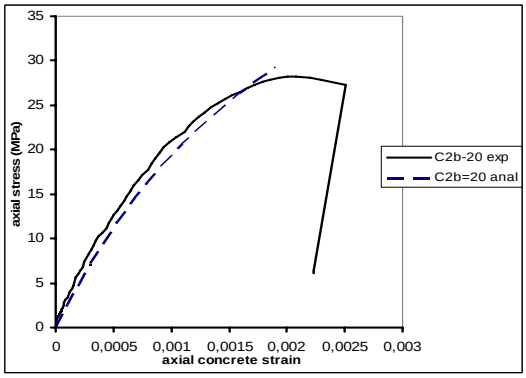

Specimen C2b-20

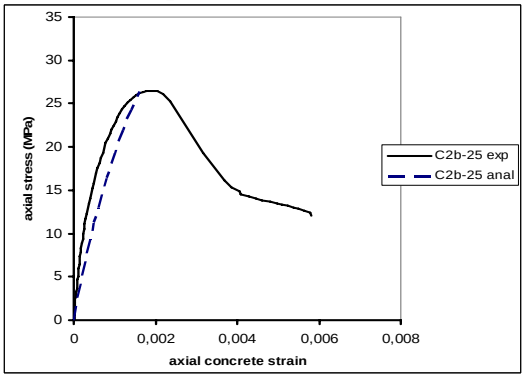

Specimen C2b-25

Fig. (9): Analytical Modeling for the Axial Stress-Strain (continued)

9. Conclusions

Based on the experimental and analytical analysis of the current study, it can be concluded that :

- Confinement of rectangular columns with circular GFRP tubes or rings imbedded inside the column generally leads to improvement of the ductility of the columns as well as the axial load carrying capacity especially for the square columns. The highest improvement level is achieved for the case of columns with continuous tubes.
- Square columns recorded increase in the ductility with confinement while for rectangular columns generally lesser ductility is recorded.

- Rectangular columns showed smaller strength gain and confinement factor compared to square columns.
- The slightly modified model of Fam and Rizkalla was capable to accurately predict the ascending part of the axial stress-strain curve.
- The model of Fardis and Khalili gives the best prediction for the ultimate confined strength while the model of Karbhari et al. gives the best prediction for the strain at peak confined strength.
- The strength measures, as defined above, are generally increased due to confining with the maximum increase attained by the columns with 1300 mm GFRP tubes length.

Acknowledgments

The authors wish to thank "Future Pipe Industry" for providing the GFRP tubes and rings.

References

Fam, A. Z.; and Rizkalla, S. H., 2001a. Confinement Model for Axially Loaded Concrete Confined by Circular Fiber-Reinforced Polymer Tubes, ACI Structural Journal, V. 98, No.4, 451-461.

Fam, A. Z.; and Rizkalla, S. H., 2001b. Behavior of Axially Loaded Concrete-Filled Circular Fiber-Reinforced Polymer Tubes, ACI Structural Journal, V. 98, No. 3, 280-289.

Saafi, M.; Toutanji, H. A.; and Li, Z., 1999. Behavior of Concrete Columns Confined with Fiber Reinforced Polymer Tubes, ACI Materials Journal, V. 96, No. 4, 500-510.

Mander, J. B.; Priestley, M. J. N.; and Park, R., 1988. Theoretical Stress-Strain Model for Confined Concrete, Journal of Structural Engineering, V. 114, No. 8, 1804-1826.

Karabinis, A. I., and Kiousis, P. D., 1996. Strength and Ductility of Rectangular Concrete Columns a Plasticity Approach, Journal of Structural Engineering, ASCE, V. 122, No. 3, 267-274.

Fafitis, A., and Shah, S. P., 1985. Prediction of Ultimate Behavior of Confined Columns Subjected to Large Deformations, ACI Structural Journal, V. 82, No. 4, 423-433.

Priestly, M. J. N., and Park, R., 1987. Strength and Ductility of Concrete Bridge Columns under Seismic Loading, ACI Structural Journal, 61-76.

Sheikh, S. A., and Yeh, C. C., 1986. Flexural Behavior of Confined Concrete Columns, ACI Structural Journal, V. 83, No. 3, 389-404.

Abdel-Halim, M. A. H., and Abu-Lebdeh, T. M., 1989. Analytical Study for Concrete Confinement in Tied Columns, Journal of Structural Engineering, ASCE, V. 115, No. 11, 2810-2828.

Sayed, M. S., 2005a. Feasibility of Utilizing Waste GFRP Pipes As Lateral Reinforcement for Rectangular Reinforcement Concrete Short Columns, HBRC Journal, V. 1, No. 2, 35-50.

Sayed, M. S., 2005b. Recycling Of Factory Rejected GFRP Pipes As Transverse Reinforcement For Reinforced Concrete Short Circular Columns, Proceeding Of The Forth Middle East Symposium For Composite Materials In Infrastructure Applications, Alexandria, Egypt.